*Geological Survey of Japan Cruise Report No. 21, p. 56–83, 1986*

# VI. DEEP-SEA SEDIMENTS IN THE CENTRAL EQUATORIAL PACIFIC (GH81-4 AREA)

*Akira Nishimura*

## Introduction

For the classification of the origin of the variations in morphology and abundance of manganese nodules, sedimentary history inferred from the sediment sequences gives important informations. In this chapter, lithology of the sediment samples collected during the GH81-4 Cruise is described and the construction of the sedimentary history of the survey area is attempted.

The survey area (GH81-4 area) is a small square area (60 × 70 km) situated in the central part of the Central Pacific Basin bordered by the latitudes, 2°45'N and 3°25'N, and the longitudes, 169°20'W and 169°50'W. The topography of the survey area is characterized by almost flat floor basin with 5,500–5,650 meters depth and some small abyssal hills with elevations of several hundred meters (Fig. VI-1).

Sampling methods of the sediments including manganese nodule collection used in this paticular study are as follows (Table VI-1).

Double spades box corer at 12 sites

Piston corer with an 8 m core barrel at 13 sites

Freefall grab with a small sediment sampling tube at 125 sites

Dredge at one site

Sediments collected by a box corer and a piston corer were treated in the same way as the previous works (NISHIMURA, 1980). Lithology of the sediments was determined through the smear slide observations and the sediment classification was made following the same scheme in the previous studies (NISHIMURA, 1980 and 1984) (Table VI-2). Age estimation of the sediment samples is based on the micropaleontological data (Supplement 1, this chapter) and a study of remanent magnetism of the sediment sequences (YAMAZAKI, this cruise report) correlated to a standard magnetic polarity time table (HARLAND *et al.*, 1982).

## Surface sediments

Surface sediments in the pelagic environment such as the present study area are controlled mainly by the water depth related to the Calcium Carbonate Compensation Depth (CCD) and the productivity in the surface water column. The water depth of the survey area is below the CCD situated at ca. 4,900 m (BERGER *et al.*, 1976). The situation of this area is near the high productivity zone along the equator. Reflecting these conditions, the surface sediments of the survey area collected in the top of a piston corer and a box corer and in a sediment tube attatched to a freefall grab sampler, are dark brown (10YR3/3) siliceous clay with high abundance of siliceous organism tests, mainly of radiolarians. According to the lithologic facies divisions based on the transect sediment sampling works in the Central Pacific Basin (NAKAO and MIZUNO, 1982), this area belongs to 'Equatorial siliceous biogenic zone' characterized by

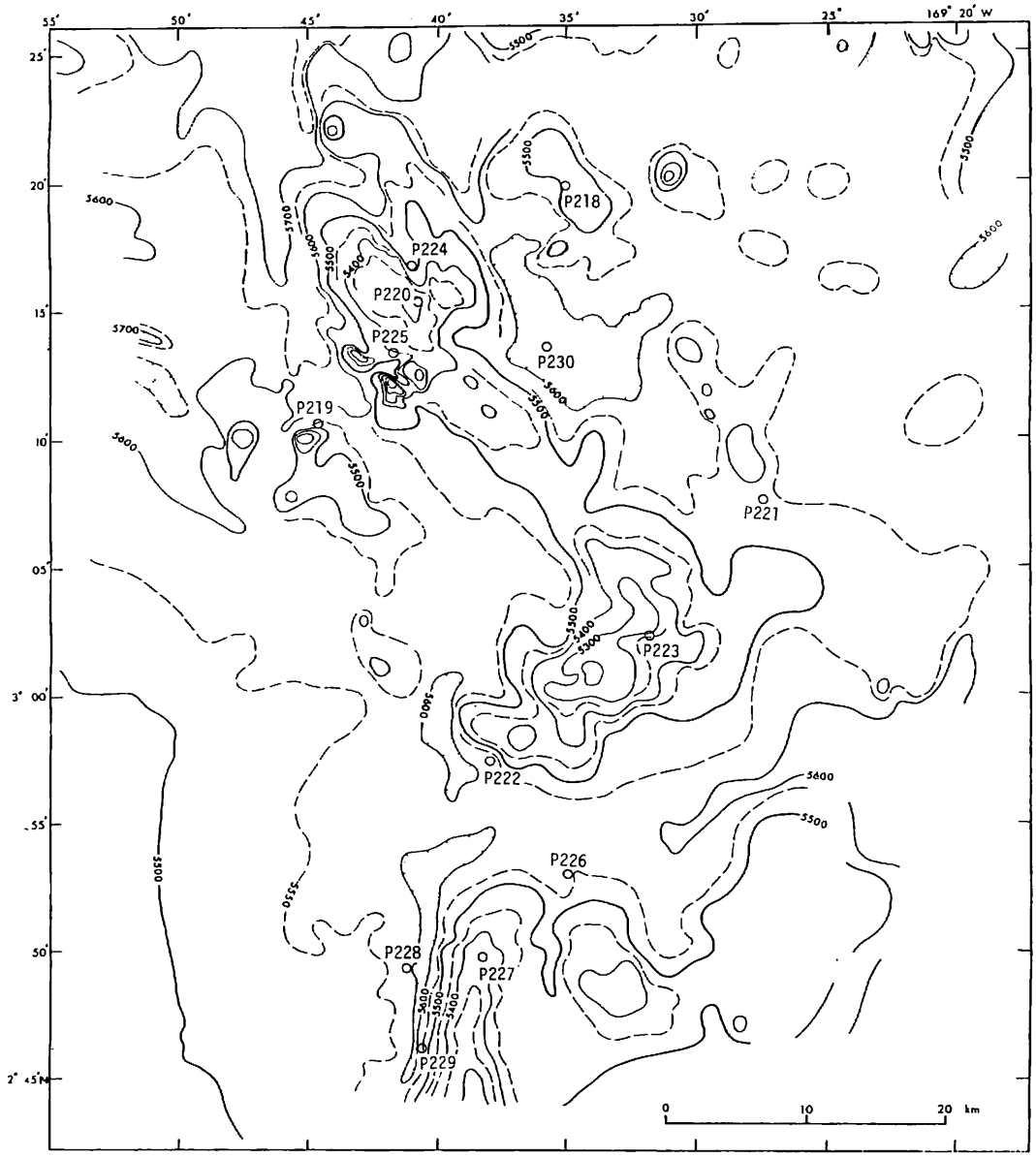


Fig. VI-1 Topography and sampling sites. Depth in meters.

Table VI-1 Sampling site data during the GH81-4 Cruise.

| Station No. | Sample No. | POSITION | | Water depth |
|---|---|---|---|---|
| | | Lat.(N) | Long.(W) | ( m ) |
| St. 2579 | P 218 | 3°19.86' | 169°35.06' | 5473 |
| 2586 | P 219 | 3°10.57' | 169°44.69' | 5578 |
| 2583 | P 220 | 3°15.30' | 169°40.79' | 5371 |
| 2591 | P 221 | 3°07.54' | 169°27.57' | 5538 |
| 2600 | P 222 | 2°57.39' | 169°38.05' | 5584 |
| 2596 | P 223 | 3°02.32' | 169°31.94' | 5309 |
| 2651 | P 224 | 3°16.64' | 169°41.07' | 5500 |
| 2663 | P 225 | 3°13.32' | 169°41.65' | 5427 |
| 2676 | P 226 | 2°53.08' | 169°34.86' | 5547 |
| 2688 | P 227 | 2°49.81' | 169°38.42' | 5355 |
| 2700 | P 228 | 2°49.29' | 169°41.20' | 5568 |
| 2712 | P 229 | 2°46.16' | 169°40.25' | 5646 |
| 2675 | P 230 | 3°13.38' | 169°35.66' | 5600 |
| 2613 | B 57 | 3°17.50' | 169°38.16' | 5605 |
| 2618 | B 58 | 3°20.61' | 169°36.16' | 5483 |
| 2622 | B 59 | 3°16.39' | 169°41.26' | 5486 |
| 2628 | B 60 | 3°18.23' | 169°44.94' | 5588 |
| 2634 | B 61 | 3°12.13' | 169°41.96' | 5461 |
| 2645 | B 63 | 3°17.49' | 169°41.71' | 5628 |
| 2657 | B 64 | 3°14.59' | 169°41.61' | 5368 |
| 2669 | B 65 | 3°14.14' | 169°40.86' | 5368 |
| 2681 | B 66 | 2°48.21' | 169°38.93' | 5360 |
| 2695 | B 67 | 2°47.29' | 169°40.28' | 5620 |
| 2705 | B 68 | 2°50.91' | 169°35.69' | 5514 |
| 2713 | D496 (hit) | 3°14.99' | 169°40.09' | 5365 |
| | (off) | 3°15.75' | 169°42.55' | 5304 |

Table VI-2 Framework of sediment classification.

| PELAGIC CLAY<br>*zeolite, siliceous fossil, and calcareous fossil*<5% | | |
|---|---|---|
| ZEOLITE RICH CLAY<br>5%<*zeolite*<10% | SILICEOUS FOSSIL RICH CLAY<br>5%<*siliceous fossil*<10% | CALCAREOUS FOSSIL RICH CLAY<br>5%<*calcareous fossil*<10% |
| ZEOLITIC CLAY<br>10%<*zeolite* | SILICEOUS CLAY<br>10%<*siliceous fossil*<30% | CALCAREOUS CLAY<br>10%<*calcareous fossil*<30% |
| | SILICEOUS OOZE<br>30%<*siliceous fossil* | CALCAREOUS OOZE<br>30%<*calcareous fossil* |

*siliceous fossil*; radiolarians, silicoflagellates, and sponge spicules
*calcareous fossil*; foraminifers and calcareous nannoplanktons

siliceous mud and siliceous ooze. No distinct difference is detected on surface sediments among the sampling sites over the survey area. In some box core sequences (Box cores B59, B61, and B63), calcareous sediments are observed at tens centimeters below the surfaces (Fig. VI-3). These sites are also far deeper than CCD at present. These sediments are thought to have been formed through the pelagic sedimentation during the fluctiation of CCD such as lowering below 5,400 meter depth level during the late Pleistocene. This is because the sedimentary structures of the calcareous sediment show no sign of turbidite origin and because the lowest part of the box core B63 below the calcareous sediments yields radiolarian species *Buccinosphaera invaginata* HAECKEL, the first appearance of which is dated to the late Pleistocene (ca. 0.2 Ma) (KNOLL and JOHNSON, 1975).

**Core sequences of the basin**

In the survey area, relatively large three abyssal hills (northern, central, and southern) are arranged in N-S direction. From the basin floor including the foot of the hills, six piston cores were taken. The homogenuity of the lithology of the core sequences and measurements of remanent magnetism of the core sequences corresponding to the standard magnetic polarity change during the Pleistocene age, show continuous sedimentation in all cores of the basin area. The ages of the lowest part of cores vary from the latest Pliocene (between the end of of the Gauss Epoch and the Olduvai Event) to the middle Pleistocene (slightly earlier than the Jaramillo Event). The sedimentation rate through the Brunhes Epoch varies from 3 to 6 mm/k.y. and the peculiar high sedimentation rate (5-9 mm/k.y.) around the Jaramillo Event with a rate about twice of that in the Brunhes Epoch, is revealed through the magnetic stratigraphy (YAMAZAKI, this cruise report). The high sedimentation rate around the Jaramillo Event is observed in the pelagic clay sediment area of the northern vicinity of the Magellan Trough, north of this area (JOSHIMA and NISHIMURA, 1984). Brief descriptions of individual core sequences are given below (Fig. VI-2).

Core P230 (the east of the northern hill): This core is composed of dark brown

siliceous clay throughout the sequence. The lowest part of the core is highly mottled. The age of the core is the Quaternary (The age of this core is from slightly after the Olduvai Event to the Recent.)

Core P221 (the northeast of the central hill): This core is composed of siliceous clay throughout the sequence. The color of the upper part is dark brown but that of the lower part is very dark grayish brown. The age of this core is from the latest Pliocene to the Recent (The base of the core is between the end of the Gauss Epoch and the Olduvai Event.)

Core P226 (the northeast of the southern hill): This core is composed of dark brown siliceous clay poorly mottled. The sedimentation rate of this core is largest among the cores taken from this area. The age of this core is the Quaternary (The base of the core is between the Olduvai Event and the Jaramillo Event.).

Core P222 (the southwestern foot of the central hill): This core is composed of dark brown siliceous clay throughout the sequence. The age of the core is from the latest Pliocene to the Recent (The base of the core is between the end of the Gauss Epoch and the Olduvai Event.).

Core P228 (the west of the southern hill): This core is composed of dark brown siliceous clay throughout the sequence. Mottled part is more distinct in the lower half than the upper half. The age of this core is almost the same as that of Core P222.

Core P229 (the western foot of the southern hill): Manganese nodules were taken from the top of this core. This core is composed of dark brown siliceous clay moderately mottled. The age of this core is the Quaternary (The age of this core is from the age immediately after the Olduvai Event to the Recent.).

**Core sequences of the hill**

Cores taken from the topographic highs of the survey area were collected from the three major hills and two small hills neighbouring the northern hill. The topographic features are as follows.

Small hill northeast of the northern hill (Core P218): This hill is located northeast of the northern hill and has NW-trending ridge with ca. 100 meters height.

Small hill southwest of the northern hill (Core P219): This hill is located southwest of the northern hill and has a peak with ca. 300 meters height.

The northern hill (Cores P220, P224, and P225, Box cores B60 and B64): In the survey area, samplings were concentrated on this hill to clarify the detailed distribution of manganese nodules. This hill has NW-trending ridge with the peak of 5,300 m in depth. Three piston cores and five box cores were taken from the hill during this cruise. One other piston core (Core P174) had been taken during the GH80-1 Cruise on the hill (3° 16.31'N, 169° 40.25'W, 5,320 m) and the presence of hiatus with duration from the early Miocene to the Pleistocene was revealed through the micropaleontology and the magnetic study (TAKAYANAGI *et al.*, 1982 and JOSHIMA, 1982).

The central hill (Core P223): This hill is located in the central part of the survey area and has NE-trending ridge with a peak of 5,200 meters in depth. Along the southwestern margin of the hill, deep moat is present.

The southern hill (Core P227): This hill has ridge with N–S axis and deep moat along the western foot of the hill. E–W traversed survey was carried out to clarify the

distribution of manganese nodules.

On the hills, air gun record shows thinner transparent layers than those on the basin, which is probably related to hiatus development and slow deposition on topographic highs. All piston cores and two box cores (Box cores B60 and B64) taken from the hill area have hiatuses in the sequences (Figs. VI-2 and VI-3). Almost hiatuses are detected by the lithological change through the visual description and the smear slide observation and the durations of hiatus are determined through the micropaleontology (Supplement 1, this chapter) and magnetic stratigraphy (YAMAZAKI, this cruise report). The uppermost hiatus presents near the surface shallower than one meter except Cores P224 and P225, and the sediments above the hiatus is composed of dark brown siliceous clay as the same as the surface sediments in the basin which is late Pleistocene to recent deposits. The rests of the core below the hiatus are mainly composed of siliceous ooze with highly abundant radiolarians. The brief descriptions of core lithologies including the hiatuses in the sequences are as follows (Fig. VI-2).

Core P218: This core has a hiatus at 12 cm from the top. The sediments above the hiatus is composed of dark brown siliceous clay, and that below the hiatus of dominantly dark brown siliceous ooze moderately mottled of the Pliocene age (from the late Gilbert Epoch to the end of Gauss Epoch). Two black manganese micronodule concentrated layers (4 and 5 cm in thickness) are intercalated in the uppermost part of the lower lithologic unit (Supplement 2, this chapter).

Core P219: This core has a hiatus at 10 cm from the top. The lithology above the hiatus is composed of dark brown siliceous clay and that below the hiatus of dark brown pelagic clay in the upper part and dark brown siliceous ooze in the lower part. The age of the sediment sequence below the hiatus is mostly the same as that of Core P218 (from the middle Gilbert Epoch to the end of the Gauss Epoch). The age of the pelagic clay part forming the upper part of the sequence below the hiatus is correlative to the Gauss Epoch.

Core P220: This core has a hiatus at 16 cm from the top. The lithology above the hiatus is composed of dark brown siliceous clay and that below the hiatus of brown siliceous ooze. The age of the lower lithologic unit is assigned to the middle Miocene (ca. 14.5-8.5 Ma). The change of sedimentation rate drawn on the correlation of magnetic stratigraphy shows the very slow sedimentation around ca. 12 Ma which represents the possibility of short hiatus (ca. 0.5 m.y.) there. In the core sequence, *zoophycos* is dominant biogenic structure in the sediments. *Zoophycos* were observed in the only two core sequences of the transect survey of the Central Pacific (Cores P173 and P174) (NAKAO and MIZUNO, 1982), which were taken in and near the this survey area, and lithology of which is dominant siliceous ooze.

Core P224: This core has a hiatus at 188 cm from the top. The lithology above the hiatus is composed of dark brown siliceous clay and that below the hiatus of dark brown siliceous ooze. The magnetization above the hiatus is normal which is included in the Brunhes Epoch. The age below the hiatus is the early Miocene (Supplement 1, this chapter) but precise correlation to standard polarity changes is difficult (YAMAZAKI, this cruise report). Manganese nodule was found in the lowest part of the core.

Core P225: This core has a hiatus at 268 cm from the top. The lithology above the

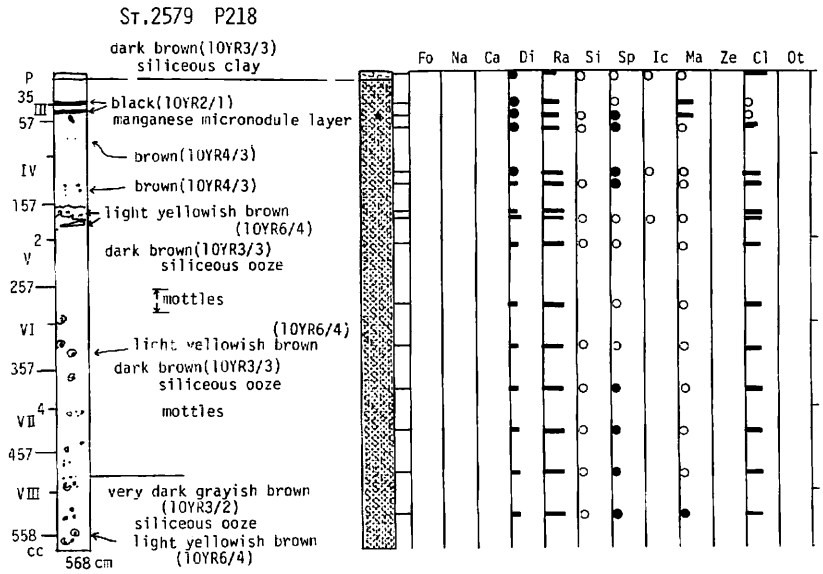


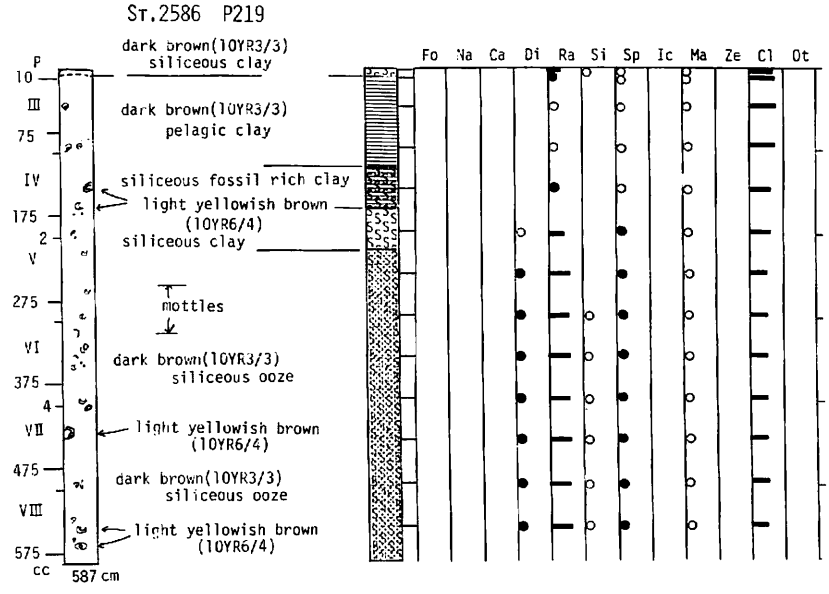


Fig. VI-2(1)

Fig. VI-2 (1)-(7). Descriptions of individual piston cores. Legend is shown in Fig. VI-2 (7).

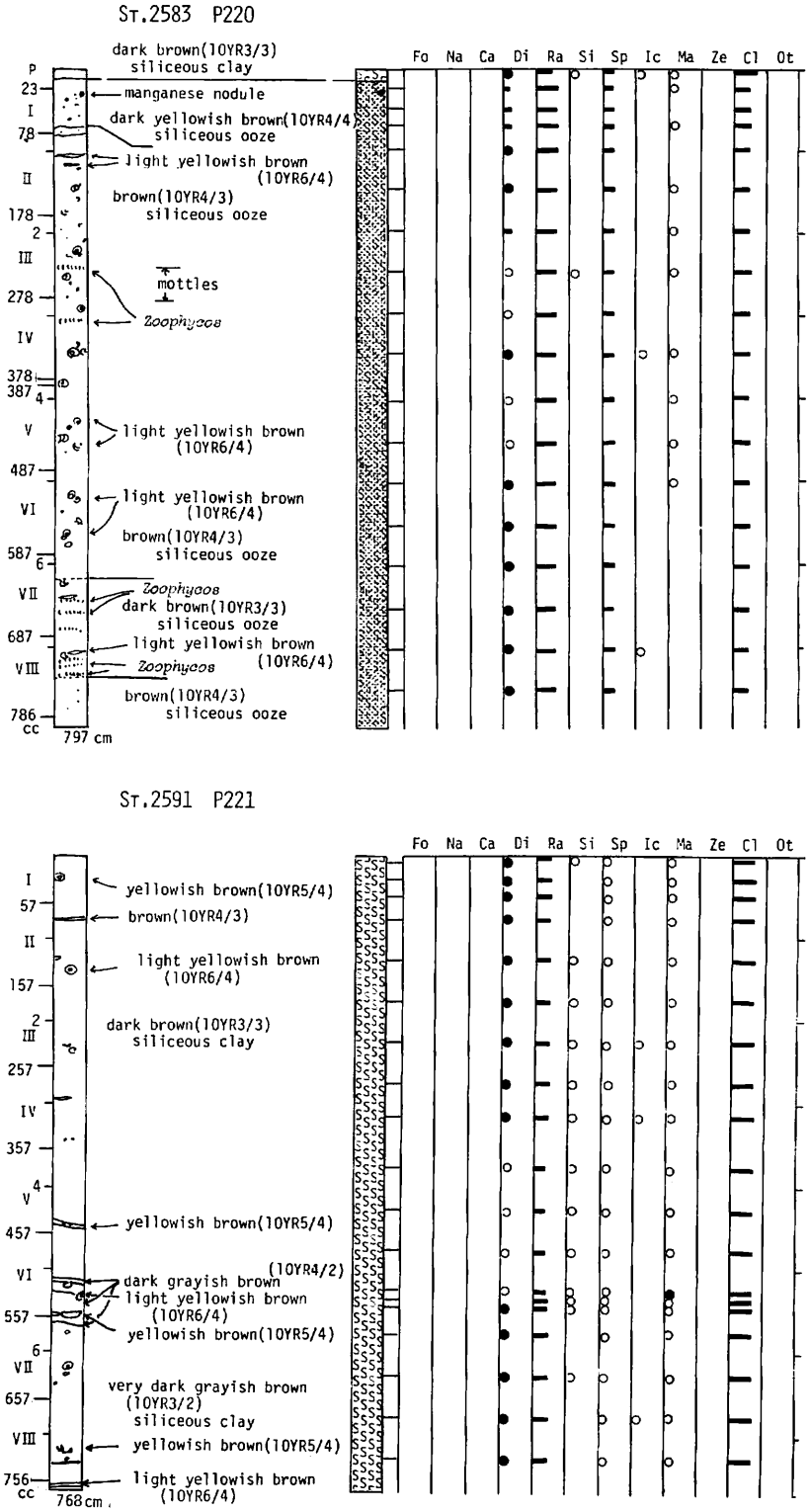
St.2583 P220
dark brown(10YR3/3)
siliceous clay
manganese nodule
dark yellowish brown(10YR4/4)
siliceous ooze
light yellowish brown
(10YR6/4)
brown(10YR4/3)
siliceous ooze
mottles
Zoophycos
light yellowish brown
(10YR6/4)
light yellowish brown
(10YR6/4)
brown(10YR4/3)
siliceous ooze
Zoophycos
dark brown(10YR3/3)
siliceous ooze
light yellowish brown
(10YR6/4)
Zoophycos
brown(10YR4/3)
siliceous ooze
797 cm
Fo Na Ca Di Ra Si Sp Ic Ma Ze Cl Ot
St.2591 P221
yellowish brown(10YR5/4)
brown(10YR4/3)
light yellowish brown
(10YR6/4)
dark brown(10YR3/3)
siliceous clay
yellowish brown(10YR5/4)
(10YR4/2)
dark grayish brown
light yellowish brown
(10YR6/4)
yellowish brown(10YR5/4)
very dark grayish brown
(10YR3/2)
siliceous clay
yellowish brown(10YR5/4)
light yellowish brown
(10YR6/4)
768 cm
Fo Na Ca Di Ra Si Sp Ic Ma Ze Cl Ot

Fig. VI-2(2)

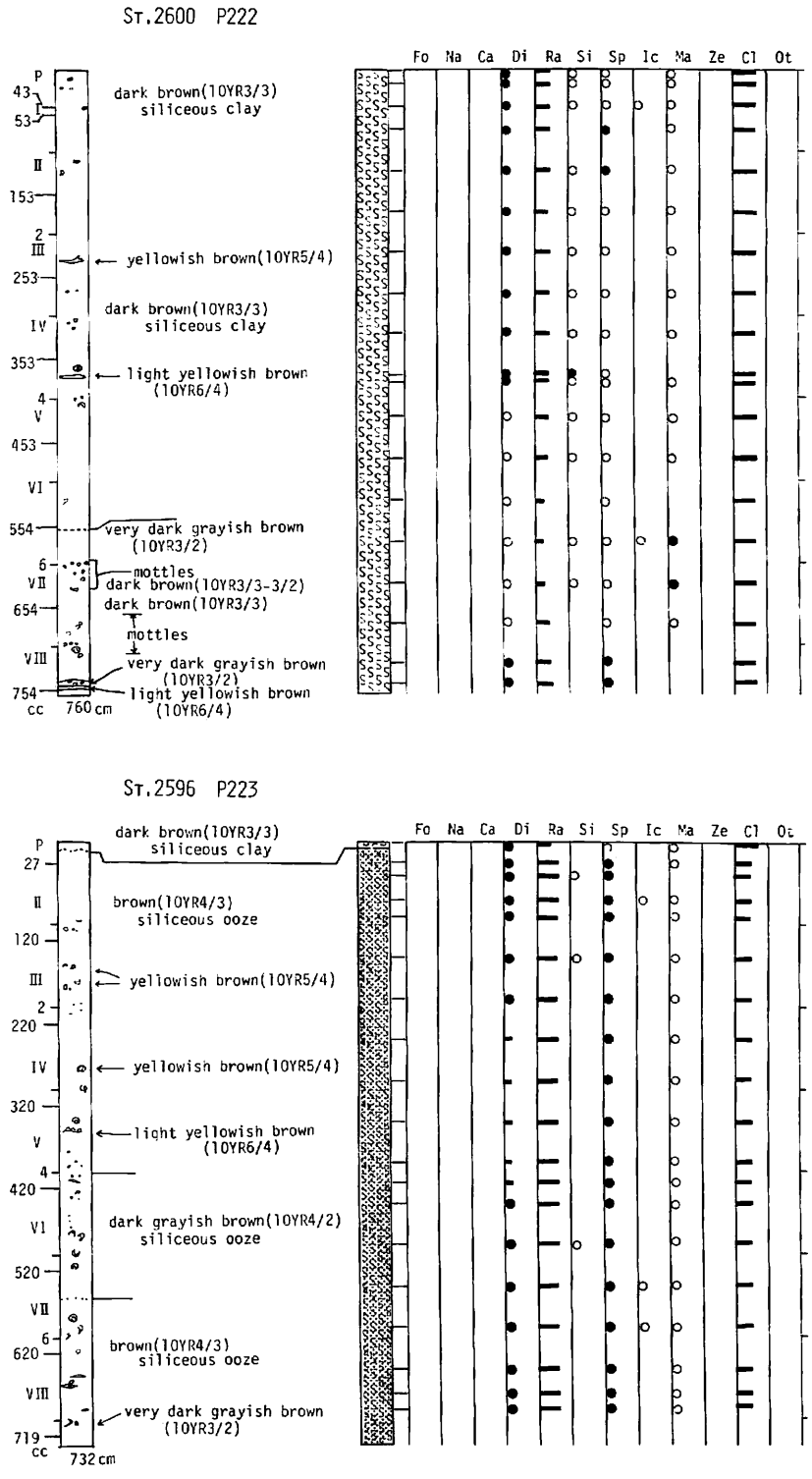
St.2600 P222
Fo Na Ca Di Ra Si Sp Ic Ma Ze Cl Ot
P
43
53
II
153
2
III
253
IV
353
4
V
453
VI
554
6
VII
654
VIII
754
cc
760cm
dark brown(10YR3/3)
siliceous clay
yellowish brown(10YR5/4)
dark brown(10YR3/3)
siliceous clay
light yellowish brown
(10YR6/4)
very dark grayish brown
(10YR3/2)
mottles
dark brown(10YR3/3-3/2)
dark brown(10YR3/3)
mottles
very dark grayish brown
(10YR3/2)
light yellowish brown
(10YR6/4)
St.2596 P223
Fo Na Ca Di Ra Si Sp Ic Ma Ze Cl Ot
P
27
II
120
III
2
220
IV
320
V
4
420
VI
520
VII
6
620
VIII
719
cc
732cm
dark brown(10YR3/3)
siliceous clay
brown(10YR4/3)
siliceous ooze
yellowish brown(10YR5/4)
yellowish brown(10YR5/4)
light yellowish brown
(10YR6/4)
dark grayish brown(10YR4/2)
siliceous ooze
brown(10YR4/3)
siliceous ooze
very dark grayish brown
(10YR3/2)

Fig. VI-2(3)

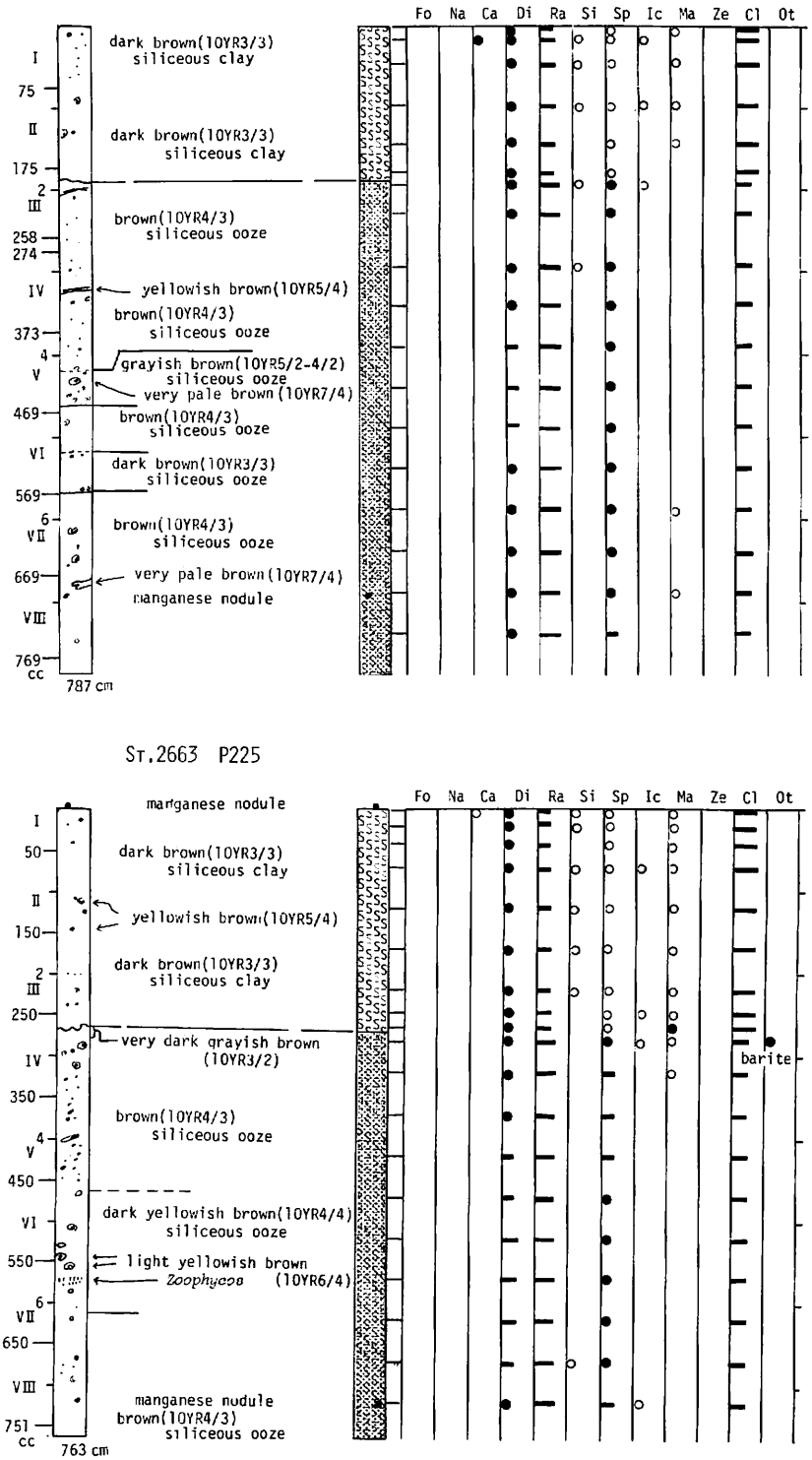
St.2651 P224
Fo Na Ca Di Ra Si Sp Ic Ma Ze Cl Ot
I
75
II
175
2
III
258
274
IV
373
4
V
469
VI
569
6
VII
669
VIII
769
cc
787 cm
dark brown(10YR3/3) siliceous clay
dark brown(10YR3/3) siliceous clay
brown(10YR4/3) siliceous ooze
yellowish brown(10YR5/4)
brown(10YR4/3) siliceous ooze
grayish brown(10YR5/2-4/2) siliceous ooze
very pale brown(10YR7/4)
brown(10YR4/3) siliceous ooze
dark brown(10YR3/3) siliceous ooze
brown(10YR4/3) siliceous ooze
very pale brown(10YR7/4)
manganese nodule
St.2663 P225
Fo Na Ca Di Ra Si Sp Ic Ma Ze Cl Ot
I
50
II
150
2
III
250
IV
350
4
V
450
VI
550
6
VII
650
VIII
751
cc
763 cm
manganese nodule
dark brown(10YR3/3) siliceous clay
yellowish brown(10YR5/4)
dark brown(10YR3/3) siliceous clay
very dark grayish brown (10YR3/2)
barite
brown(10YR4/3) siliceous ooze
dark yellowish brown(10YR4/4) siliceous ooze
light yellowish brown
Zoophycos (10YR6/4)
manganese nodule
brown(10YR4/3) siliceous ooze

Fig. VI-2(4)

St.2676 P226

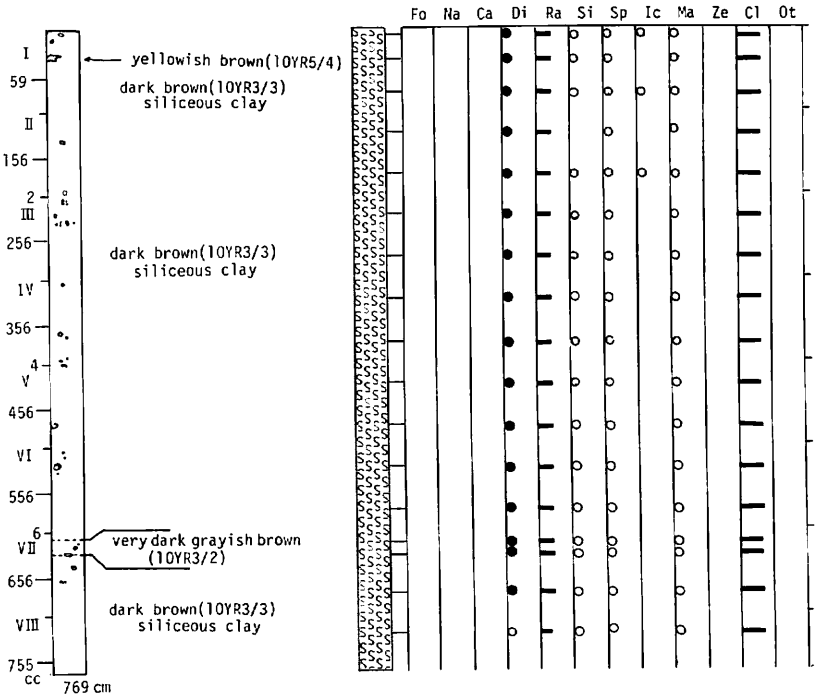


St.2688 P227

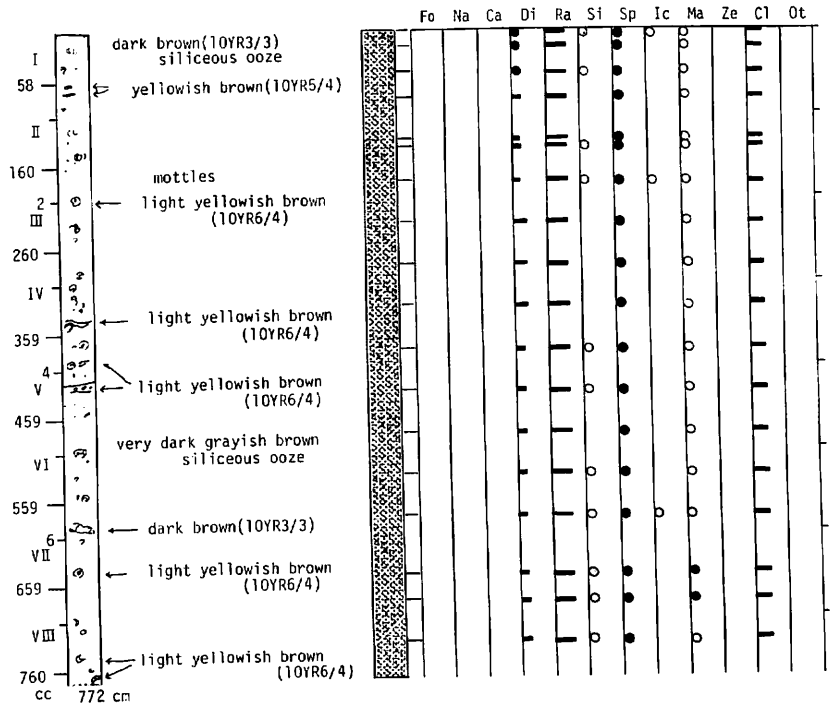


Fig. VI-2(5)

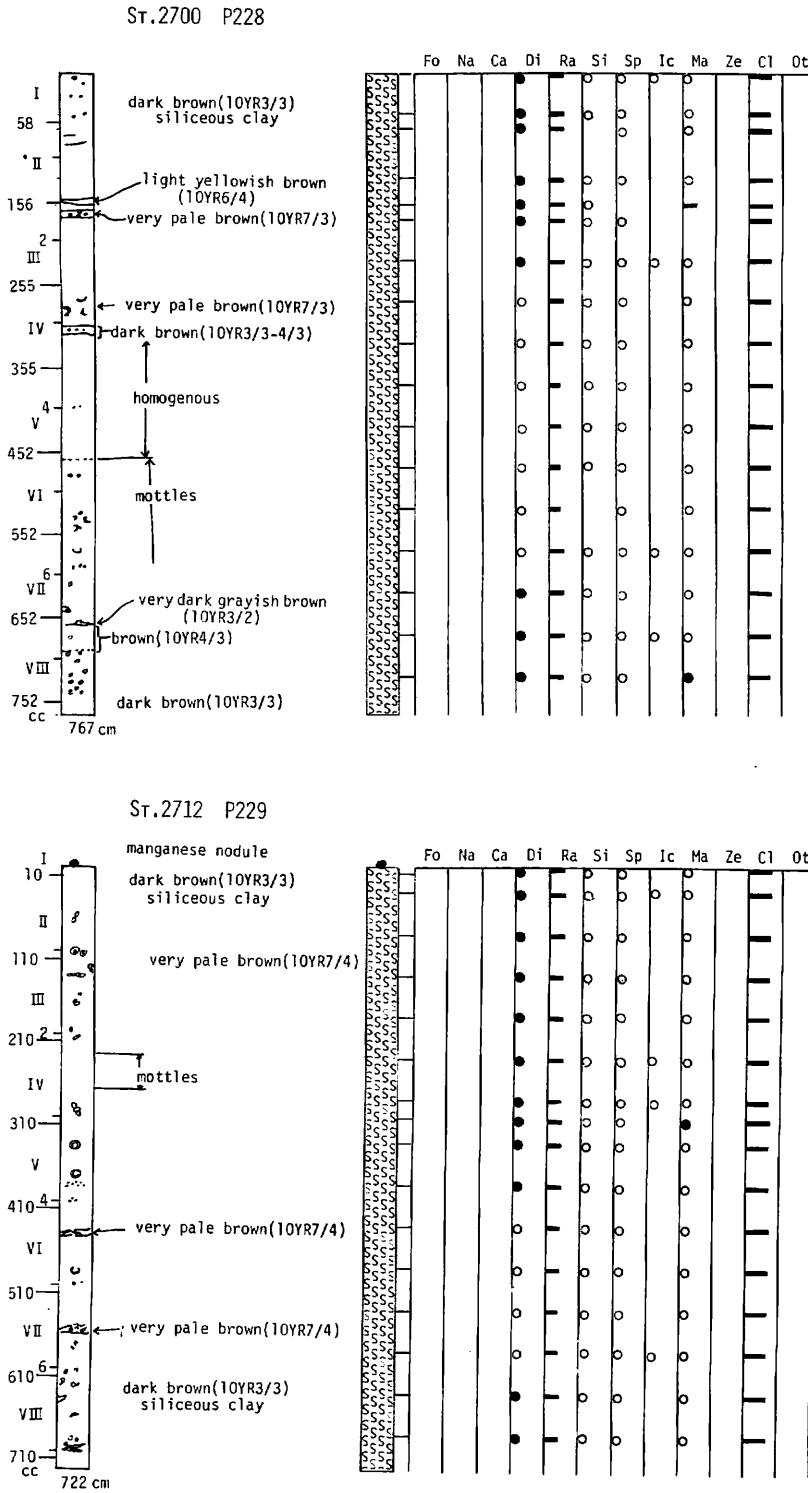
St.2700 P228
Fo Na Ca Di Ra Si Sp Ic Ma Ze Cl Ot
I
58
II
156
2
III
255
IV
355
4
V
452
VI
552
6
VII
652
VIII
752
cc
767 cm
dark brown(10YR3/3)
siliceous clay
light yellowish brown
(10YR6/4)
very pale brown(10YR7/3)
very pale brown(10YR7/3)
dark brown(10YR3/3-4/3)
homogenous
mottles
very dark grayish brown
(10YR3/2)
brown(10YR4/3)
dark brown(10YR3/3)
St.2712 P229
manganese nodule
I
10
II
110
III
210
2
IV
310
V
410
4
VI
510
VII
610
6
VIII
710
cc
722 cm
dark brown(10YR3/3)
siliceous clay
very pale brown(10YR7/4)
mottles
very pale brown(10YR7/4)
very pale brown(10YR7/4)
dark brown(10YR3/3)
siliceous clay

Fig. VI-2(6)

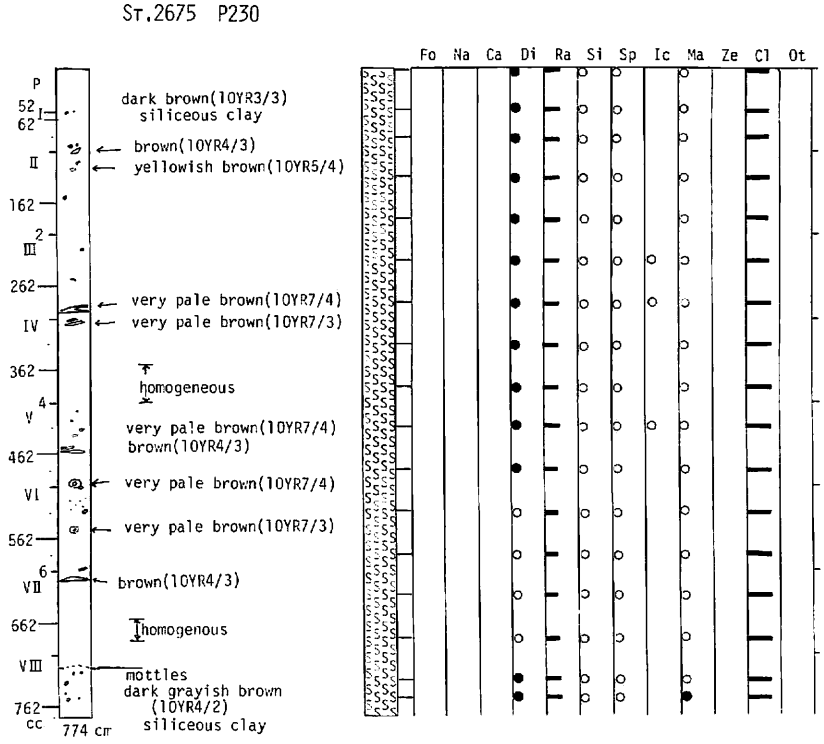


# LEGEND

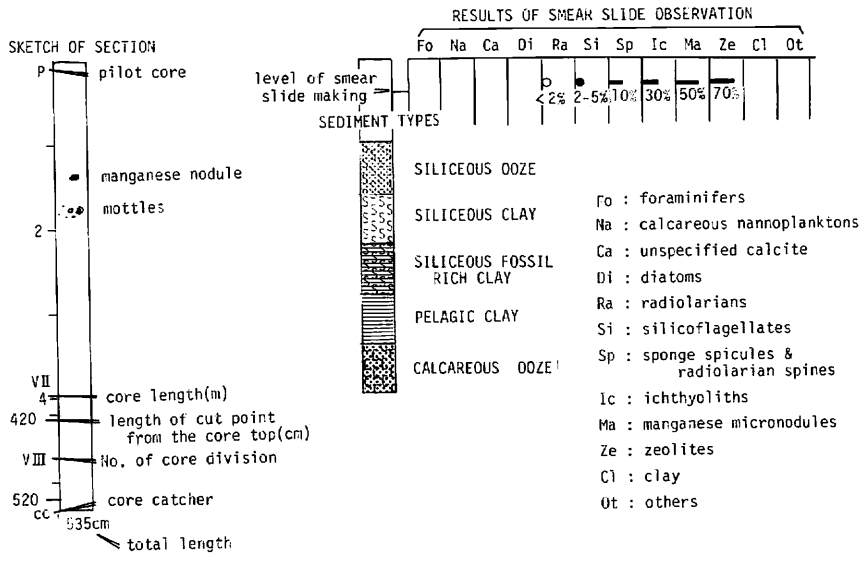


Fig. VI-2(7)

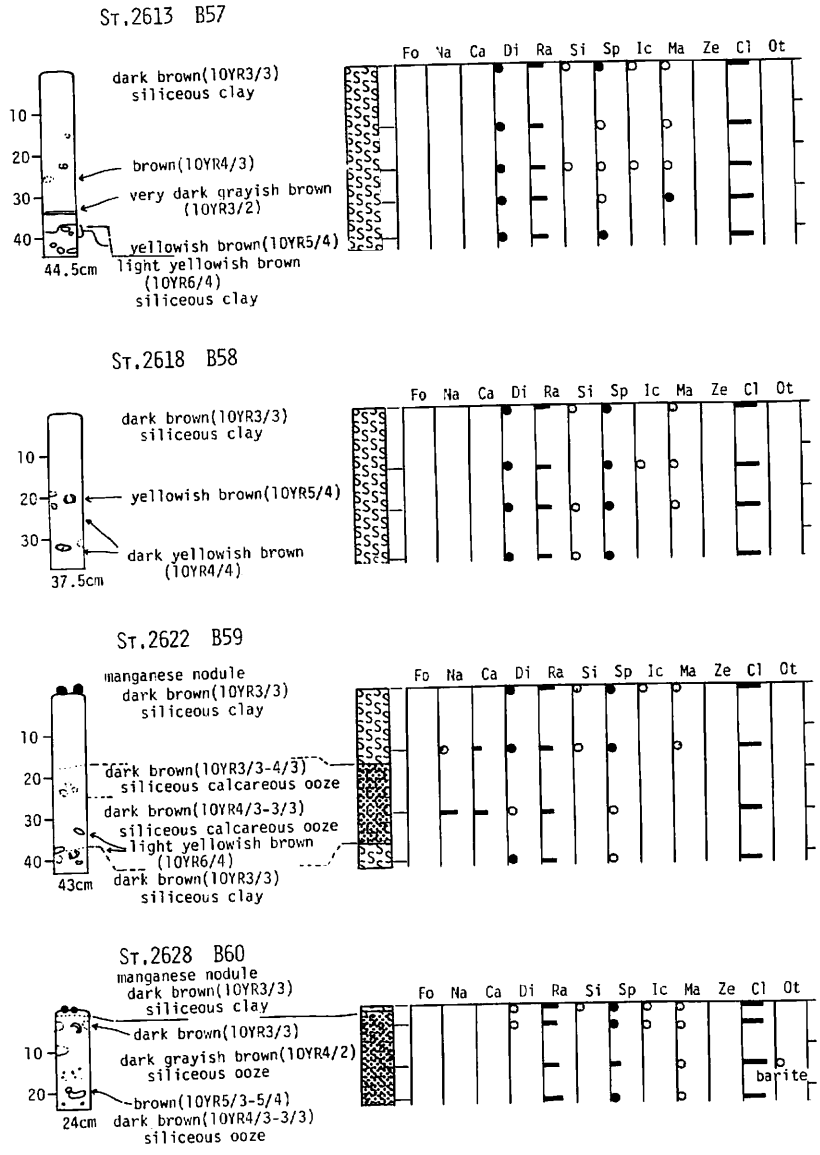


Fig. VI-3(1)

Fig. VI-3 (1)-(3). Descriptions of individual box cores. Legend is the same as that of Fig. VI-2.

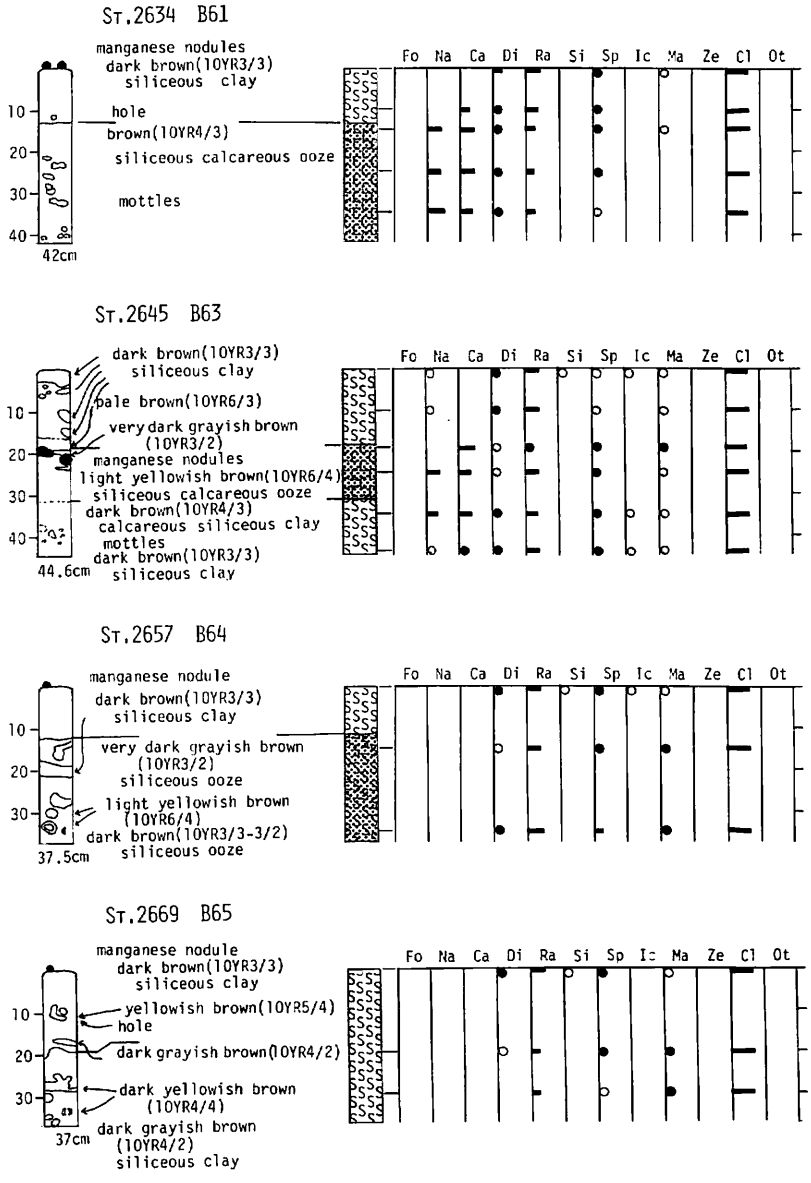
St.2634 B61
manganese nodules
dark brown(10YR3/3)
siliceous clay
hole
brown(10YR4/3)
siliceous calcareous ooze
mottles
42cm
St.2645 B63
dark brown(10YR3/3)
siliceous clay
pale brown(10YR6/3)
very dark grayish brown
(10YR3/2)
manganese nodules
light yellowish brown(10YR6/4)
siliceous calcareous ooze
dark brown(10YR4/3)
calcareous siliceous clay
mottles
dark brown(10YR3/3)
siliceous clay
44.6cm
St.2657 B64
manganese nodule
dark brown(10YR3/3)
siliceous clay
very dark grayish brown
(10YR3/2)
siliceous ooze
light yellowish brown
(10YR6/4)
dark brown(10YR3/3-3/2)
siliceous ooze
37.5cm
St.2669 B65
manganese nodule
dark brown(10YR3/3)
siliceous clay
yellowish brown(10YR5/4)
hole
dark grayish brown(10YR4/2)
dark yellowish brown
(10YR4/4)
dark grayish brown
(10YR4/2)
siliceous clay
37cm
Fo Na Ca Di Ra Si Sp Ic Ma Ze Cl Ot

Fig. VI-3(2)

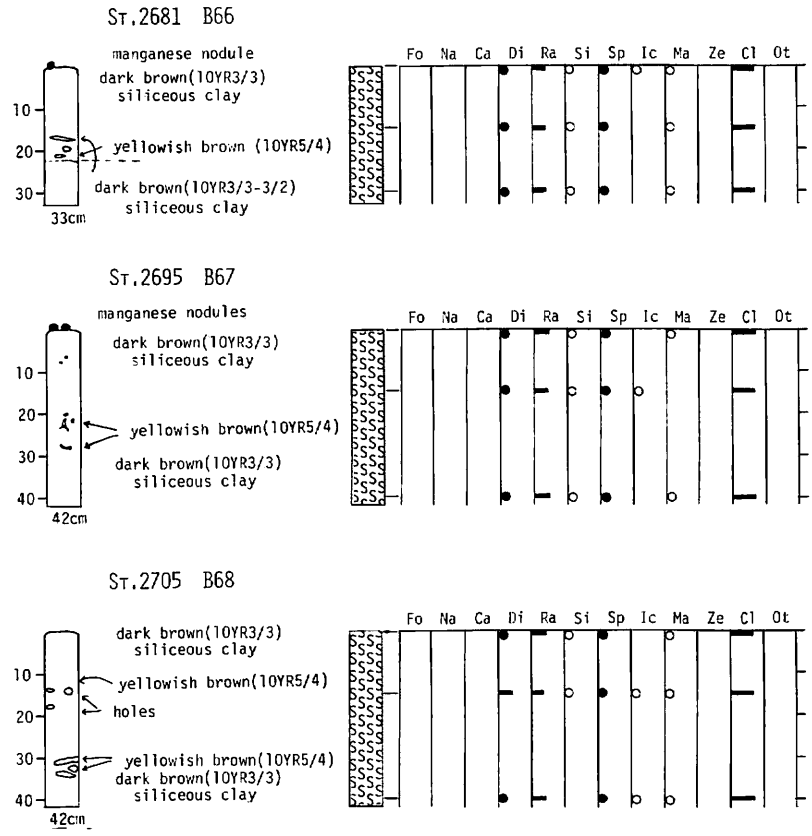


Fig. VI-3(3)

hiatus is dark brown siliceous clay and that below the hiatus of dark brown siliceous ooze. The occurrence of silicoflagellates *Mesocene quandrangula* EHRENBERG just above the hiatus and the presence of reversed magnetized part just above the hiatus assigns 0.8 Ma to the oldest age of the upper lithologic unit. The age below the hiatus is almost the same as that below the hiatus in Core P224 (the early Miocene). Siliceous ooze just below the hiatus yields barite crystals (Supplement 2, this chapter). Manganese nodules were found on the top of the core and in the lowest part of the core.

Core P223: This core has two hiatuses in the sequence. The upper hiatus present at 9 cm from the top and the lithology above the hiatus is composed of dark brown siliceous clay. The lower hiatus is present at 450 cm from the top. The lithology between two hiatuses is composed of brown siliceous ooze of the Pliocene (from the end of the Epoch 5 to the late Gilbert Epoch) and that below the lower hiatus of brown to dark grayish brown siliceous ooze of the latest middle Miocene (ca. 12–10 Ma).

Core P227: This core has two hiatuses in the sequence. The upper hiatus is present at 16 cm from the top of the pilot core. The lithology above the hiatus is dark brown siliceous clay and that below the hiatus is dark brown to very dark grayish brown

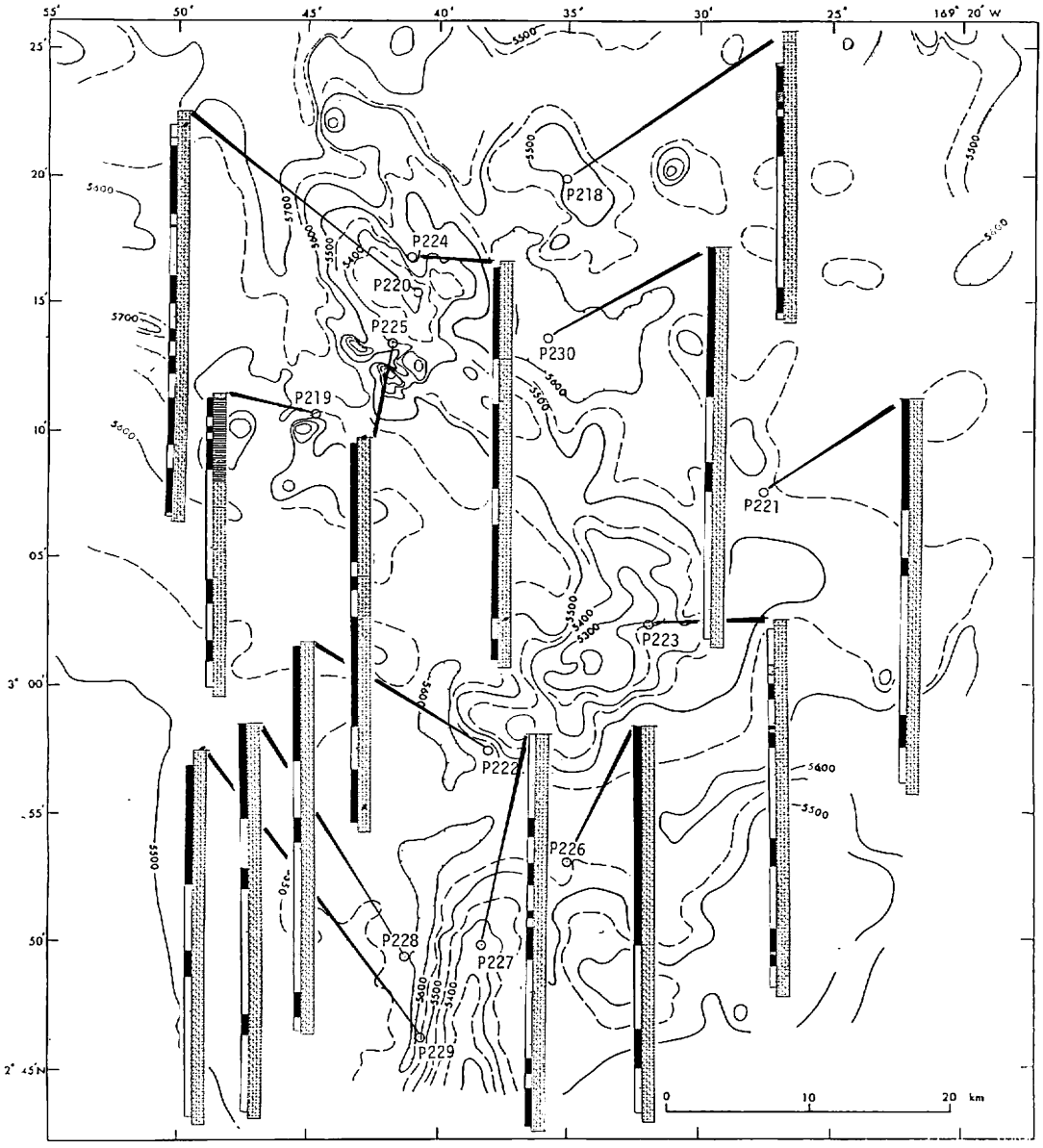


Fig. VI-4 Simplified core sequences on topographic map. Details are shown in Figs. VI-2 and VI-7.

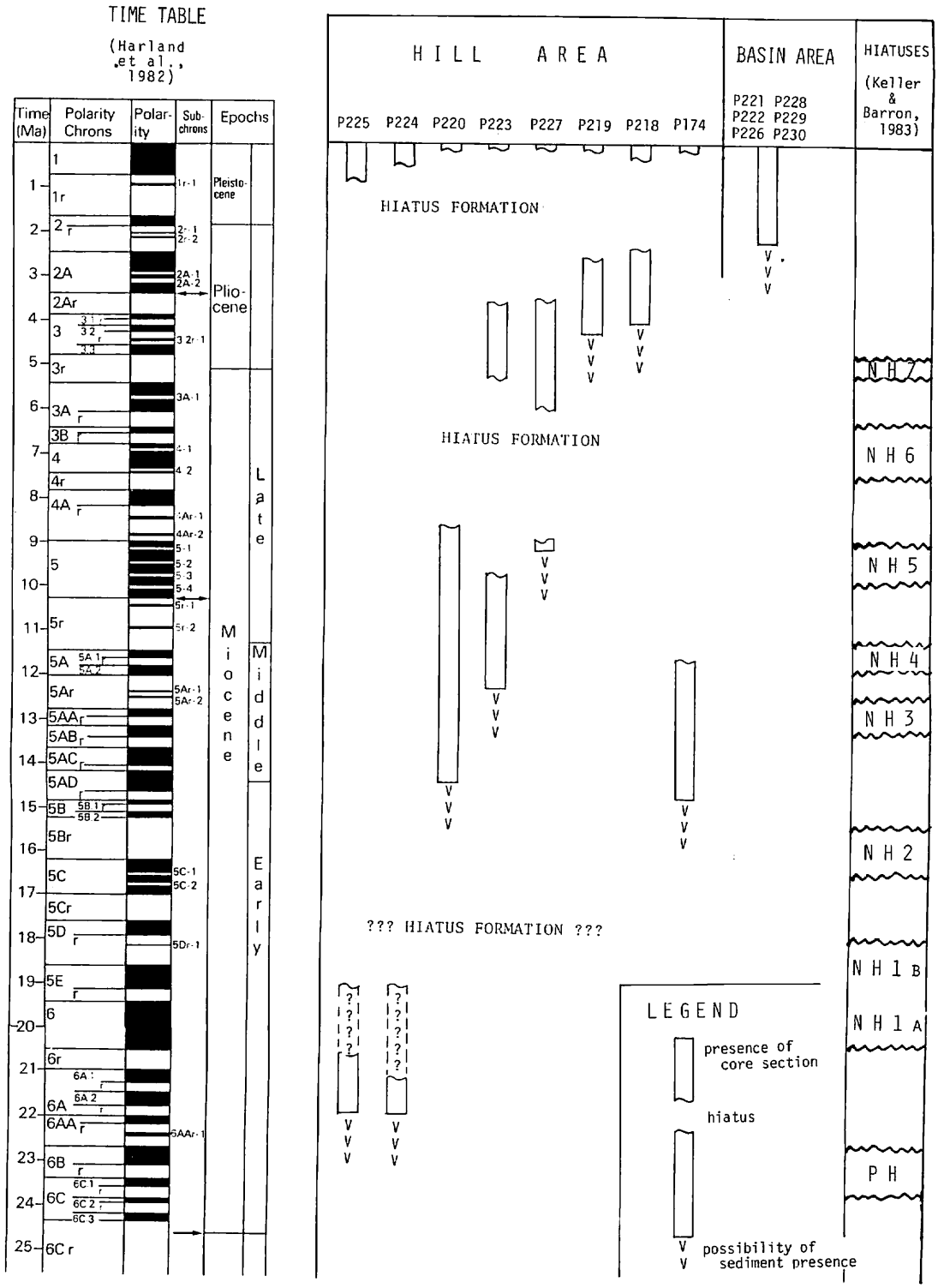


Fig. VI-5 Core sequences in time table.

siliceous ooze moderately mottled of the late Miocene (from the early Epoch 5 to the latest Gilbert Epoch). The lowest part of the core yields early late Miocene radiolarians (Supplement 1, this chapter) which suggests other hiatus in the lowest normal magnetized part of the core (YAMAZAKI, this cruise report).

Box core B60: This core has a hiatus only 2 cm below the surface. The lithology above a hiatus is dark brown siliceous clay and that below the hiatus is dark grayish brown siliceous ooze of the early Miocene.

Box core B64: This core has a hiatus 13 cm below the surface. The lithology above the hiatus is dark brown siliceous clay and that below the hiatus is dark brown siliceous ooze of the late Pliocene.

**Dredged sample of the hill**

One dredge sampling (Dredge D496) for collecting manganese nodules was tried across the summit of the northern hill. Around the sampling site, opaque layer as a basement on 3.5 kHz subbottom profiling record is exposed. At this site, thick manganese crusted (1–2 cm thick) claystone was taken with abundant manganese nodules. Claystone is creamy white to yellowish brown in color and composed of clay with ichthyoliths and manganese micronodules. The age of this claystone is the late Eocene to the Oligocene, assigned from the ichthyolith stratigraphy (Supplement 1, this chapter).

**Hiatus formation**

As already mentioned above, cores taken from the hill area have hiatuses in the sequences (Fig. VI-4). The principal cause of hiatus formation in the Central Pacific Basin is thought to be an erosion by bottom current (Antarctic Bottom Water; AABW) flowing into the basin through the Samoan Passage (HOLLISTER *et al.*, 1974 and LONSDALE, 1981) during the intensification of bottom current activity (NAKAO and MIZUNO, 1982 and NISHIMURA, 1984). As for this area, the vertical profiles of water temperature obtained at the sampling sites using heat flow measurement instrument (YAMAZAKI, this cruise report), show that the boundary between the Pacific Bottom Water (=AABW) and the Pacific Deep Water is present at ca. 4,500 meters in depth, and all sampling sites are situated in the Pacific Bottom Water. The presence of moats along the hills and mud waves (TANAHASHI, this cruise report) formed by strong influence of bottom current in recent ages suggests sedimentation under the bottom current influences. The flow direction of bottom current is thought to have been probably north-east ward based on the moat distribution along the western margins of the hills. The age of intensification of bottom current eroding the sediments are suggested by the durations of lacking the sediments on the hills, that is, 18.5 (20.5?)–15 Ma (early Miocene), 8.5–6 Ma (late Miocene), and 2.5–0.8 Ma (late Pliocene to early Pleistocene) (Fig. VI-5). The oldest duration is not sure because of short penetration of cores. The younger two durations surely have erosional times. The duration of 8.5–6 Ma which is decided by the hiatus durations in Cores P220, P223, and P227, includes the Neogene Hiatus Event, NH6, which is cleared from the DSDP research (KELLER and BARRON, 1983). The duration of 2.5–0.8 Ma is revealed by the youngest sediment below the hiatus (P225) and the oldest sediment age of above the hiatus (P225), and includes the

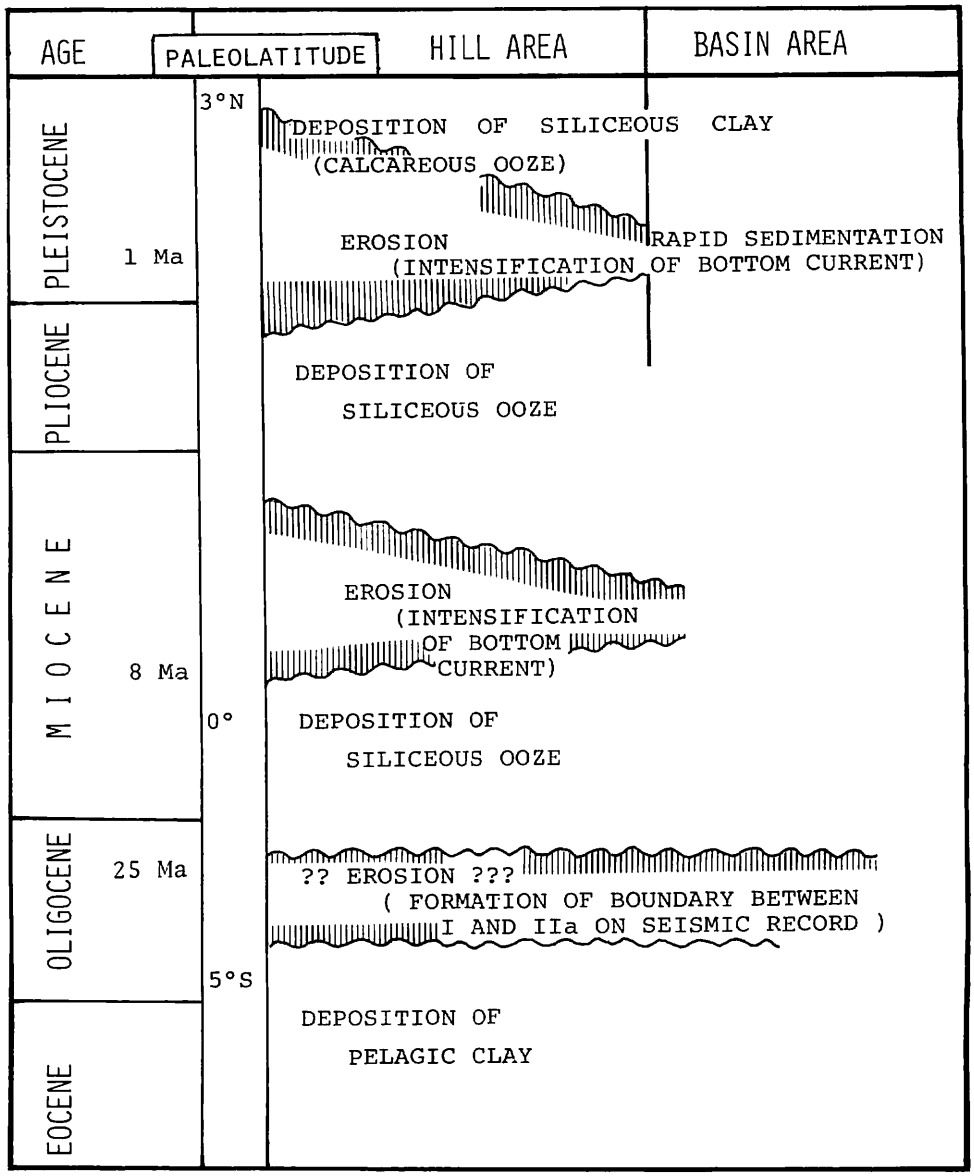


Fig. VI-6 Schematic sedimentary history in GH81-4 area.

peak of the intensification of bottom current related to formation of the youngest hiatus in this area. In this duration, high sedimentation rate around the Jaramillo Event is distinct phenomena in the basin area, which is possibly related to the erosion on the hill area. Thin covered uppermost sediments above the hiatus suggest extending erosion and/or no deposition conditions after the peak of the intensification of bottom current near to the present.

**Summary and sedimentary history**

The sediment samples obtained during the GH81-4 Cruise were described. Surface sediments composed of siliceous clay with abundant radiolarians show the pelagic sedimentation under the influence of the high productivity zone near the equator and the CCD at present.

From the lithologic data of the sediment sequences of piston cores and sedimentary rock taken by a dredge combined with micropaleontologic data and magnetic stratigraphy, the sedimentary history is constructed as follows. (Fig. VI-6).

(1) In the Paleogene, pelagic clay had been deposited. After that, the erosional event (suggested by the presence of contrast between Unit I and Unit II-A on seismic records or between transparent layer and opaque one on subbottom profiling records) probably occurred. This area is thought to have been probably situated south of southern margin of the high productivity zone along the equator in the Paleogene, considering the paleolatitude reconstructed by plate motion (VAN ANDEL *et al.*, 1975).

(2) In the Miocene through the Pliocene, siliceous ooze with highly abundant radiolarians had been deposited in the high productivity zone along the equator. The paleolatitude of this area reconstructed by plate motion is near the equator in the Miocene through the Pliocene (VAN ANDEL *et al.*, 1975).

(3) The intensified bottom water had sporadically eroded the sediments especially on the hills (at least in the late Miocene (8.5-6 Ma)).

(4) The peak of intencification of bottom current forming the uppermost hiatus on the hills has presented in the late Pliocene through the early Pleistocene. Erosion and/or no deposition condition has been presented near the recent in part of the hills.

(5) On the basin floor, continuous sedimentation of siliceous clay has been occurred at least since the latest Pliocene. The proof of the presence of hiatus in the basin floor is not obtained.

Relation between the manganese nodule genesis and the sedimentary history is not mentioned in this chapter. But occurrence of manganese nodule restricted mainly in the hill with development of hiatuses suggests preferrence occurrence of manganese nodules in slow sedimentation area with hiatus (MIZUNO *et al.*, 1980).

## References


BERGER, W. H., ADELSECK, C. G. and MAYER, L. A. (1976) Distribution of carbonate in surface sediments of the Pacific Ocean. *Jour., Geophysical Res.*, 81(15), p. 2617-2627.

HARLAND, W. B., COX, A. V., LLEWELLYN, P. G., PICKTON, C. A. G., SMITH, A. G. and WALTERS, R. (1982) A geologic time scale. Cambridge Univ. Press, Cambridge, 131p.

HOLLISTER, C. D., JOHNSON, D. A. and LONSDALE, P. F. (1974) Current-controled abyssal sedimentation: Samoan Passage, equatorial Pacific. *Jour. Geol.*, 82, p. 275-300.

JOSHIMA, M. (1982) Remanent magnetization of piston cores from the Wake-Tahiti Transect in the Central Pacific. *Geol. Surv. Japan Cruise Rept.*, no. 18, p. 276-287.

JOSHIMA, M. and NISHIMURA, A. (1984) Remanent magnetization of sediment cores in GH80-5 Survey Area. *Geol. Surv. Japan Cruise Rept.*, no. 20, p. 165-192.
KELLER, G. and BARRON, J. A. (1983) Paleocenographic implications of Miocene hiatuses. *Geol. Soc. Amer., Bull.*, 94, p. 590-613.
KNOLL, A. H. and JOHNSON, D. A. (1975) Late Pleistocene evolution of the collosphaerid radiolarian *Buccinosphaera invaginata* HAECKEL. *Micropaleontol.*, 21, p. 60-68.
LONSDALE, P. F. (1981) Drifts and ponds of reworked pelagic sediment in part of the southwest Pacific. *Marine Geol.*, 43, p. 153-193.
MIZUNO, A., MIYAZAKI, T., NISHIMURA, A., TAMAKI, K. and TANAHASHI, M. (1980) Central Pacific manganese nodules, and their relation to sedimentary history. *Proc. 12th Ann. Offshore Tech. Conf.*, Houston, 3, p. 331-340.
NAKAO, S. and MIZUNO, A. (1982) Regional sedimentologic data: the Central Pacific Wake-Tahiti Transect, GH80-1 Cruise. *Geol. Surv. Japan Cruise Rept.*, no. 18, p. 95-123.
NISHIMURA, A. (1980) Deep-sea sediments in the GH79-1 area: their geological properties. *Geol. Surv. Japan Cruise Rept.*, no. 15, p. 110-142.
——— (1984) Deep-sea sediments in the GH80-5 area in the northern vicinity of the Magellan Trough. *Geol. Surv. Japan Cruise Rept.*, no. 20, p. 67-90.
TAKAYANAGI, Y., SAKAI, T., ODA, M. and HASEGAWA, S. (1982) Micropaleontology of piston cores, Wake to Tahiti. *Geol. Surv. Japan Cruise Rept.*, no. 18, p. 238-263.
VAN ANDEL, T. H., HEATH, G. R. and MOORE, T. C. Jr. (1975) Cenozoic history and paleoceanography of the Central Equatorial Pacific Ocean. *Mem. Geol. Soc. Amer.*, no. 143, p. 1-134.

## Supplement 1.
## PRELIMINARY OBSERVATIONS ON SOME MICROFOSSILS OF THE SEDIMENT SAMPLES OBTAINED DURING THE GH81-4 CRUISE, CENTRAL PACIFIC BASIN

On the process of smear slide observations on board, age determinations were tried using smear slides for lithological studies. And after considerations on the results of paleomagnetic studies, some slides of sieved residue with 63 $\mu$m-opening sieve were supplemented to micropaleontological studies. Results of observations are useful for age determinations of core samples, combined with paleomagnetic studies (YAMAZAKI, this cruise report).

### Silicoflagellates

Silicoflagellates can be easily recognized and identified in smear slides because of their small sizes and simple shapes. Especially, *Mesocena quandrangula* EHRENBERG shows simple tetragonal shape and the acme of this species forms an important zone in

the Pleistocene Epoch. *M. quandrangula* Zone defined by upper and lower limits of occurrence of this species has short time range around the Jaramillo Event in the Matuyama Epoch (0.79–1.3 Ma) (BERGGREN *et al.*, 1980). *M. quandrangula* is observed in 7 piston core sequences. Except Core P225, core sequences with *M. quandrangula* have normal magnetized parts surely correspond to the Jaramillo Event (Fig. VI-7). *M. quandrangula* occurs in the Jaramillo Event with high abundance (over 50% of silicoflagellate flora) (Fig. VI-8). High content and high abundance of *M. quandrangula* and high sedimentation rate around the Jaramillo Event shown by magnetic study of the cores suggests a distinct bloom of *M. quandrangula* around the Jaramillo Event (ZHUZE and MUKHINA, 1973).

**Radiolarians**

The top datum of *Spongaster pentas* RIEDEL and SANFILIPPO can be easily recognized using smear slide in 4 piston cores (Fig. VI-1). The datum is determined between a horizon with coexisting of *S. pentas* and *Spongaster tetras* HAECKEL and one with only *S. tetras*. The datum is dated to 3.4 Ma in the latest Gilbert Epoch of the Pliocene (THEYER *et al.*, 1978).

The results of observations on some slides for radiolarian biostratigraphy are shown in Table VI-3. Age assignement of each sample is based on compiled radiolarian range chart using data of RIEDEL and SANFILIPPO (1978) and THEYER *et al.* (1978). Two horizons of hiatuses are predicted in Cores P223 and P227.

**Ichthyoliths**

Thick manganese crusted claystone (Sample D496) is the only sedimentary rock obtained from the basement underlying unconsolidated siliceous sediments. This claystone contains no calcareous and siliceous fossil. So, age assignment on this sample is owe to ichthyoliths, microscopic fish skeletal debris. About 40 grams of dry claystone was disaggregated by boiling with hydroperoxide. From sieved residue on 63 μm-opening sieve, ichthyoliths were picked up and enclosed on slide glass with Entellan new. Identified subtypes are *Triangle crenulate, Kite-shaped longitudinal line*, and *Triangle medium wing*. Assemblage of ichthyoliths assigns the age of claystone the late Eocene to the Oligocene, compared with the previous studies (DOYLE and RIEDEL, 1979).

## References


BERGGREN, W. A., BURCKLE, L. H., CITA, M. B., COOKE, H. B. S., FUNNELL, M. B., GARTNER, S., HAYS, J. D., KENNETT, J. P., OPDYKE, N. D., PASTOURET, L., SHACKLETON, N. J. and TAKAYANAGI, Y. (1980) Towards a quaternary Time Scale. *Quaternary Research*, 13, p. 277–302.

DOYLE, P. S. and RIEDEL, W. R. (1979) Ichthyoliths: Present status of taxonomy and stratigraphy of microscopic fish skeletal debris. *SIO Reference*, 79-16, 231p.

RIEDEL, W. R. and SANFILIPPO, A. (1978) Stratigraphy and evolution of tropical Cenozoic radiolarians. *Micropaleontology*, 23, p. 61–96.

THEYER, F., MATO, C. Y. and HAMMOND, S. R. (1978) Paleomagnetic and

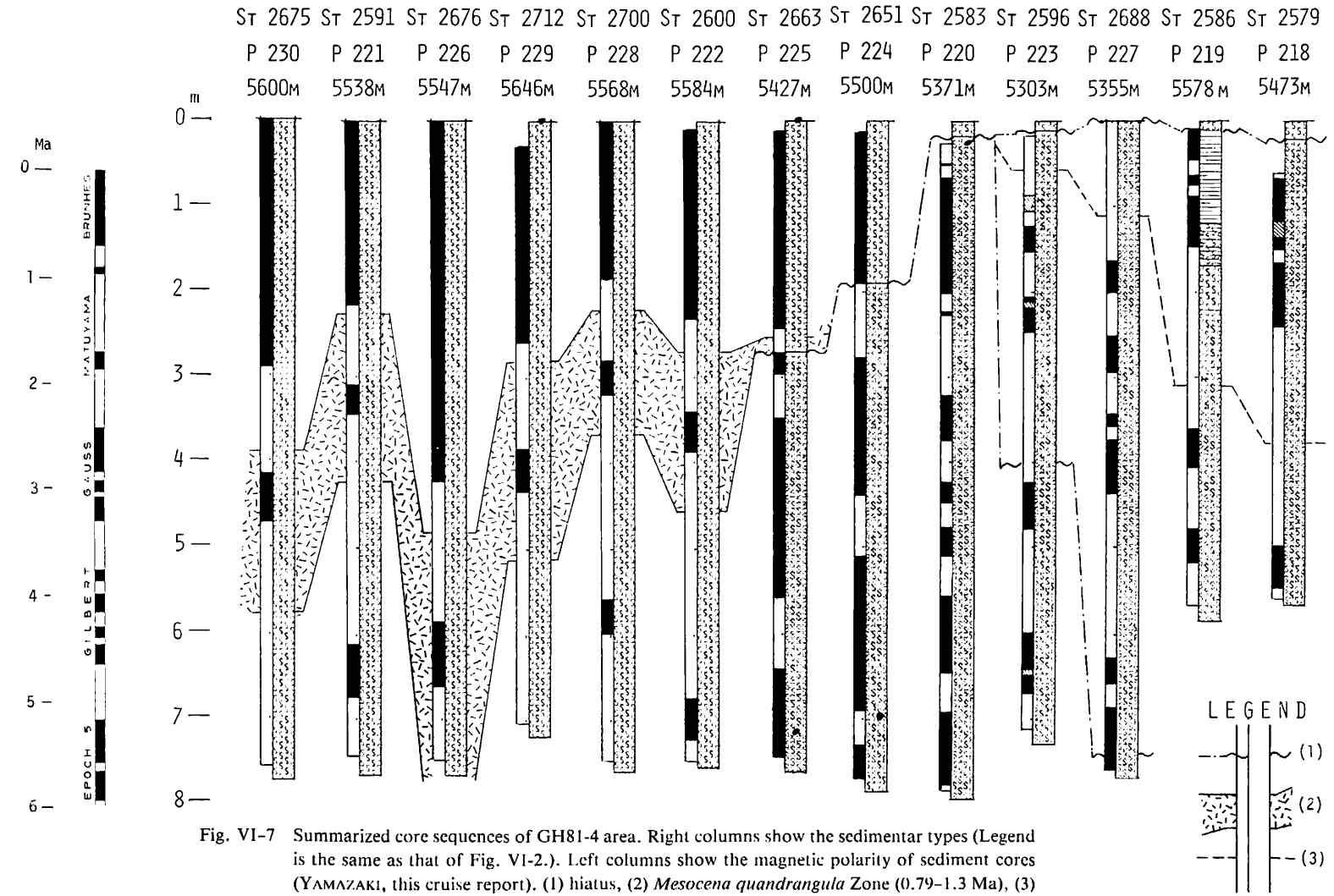


Fig. VI-7 Summarized core sequences of GH81-4 area. Right columns show the sedimentar types (Legend is the same as that of Fig. VI-2.). Left columns show the magnetic polarity of sediment cores (YAMAZAKI, this cruise report). (1) hiatus, (2) *Mesocena quandrangula* Zone (0.79–1.3 Ma), (3) top horizon of *Spongaster pentas* RIEDEL and SANFILIPPO (ca. 3.4 Ma).

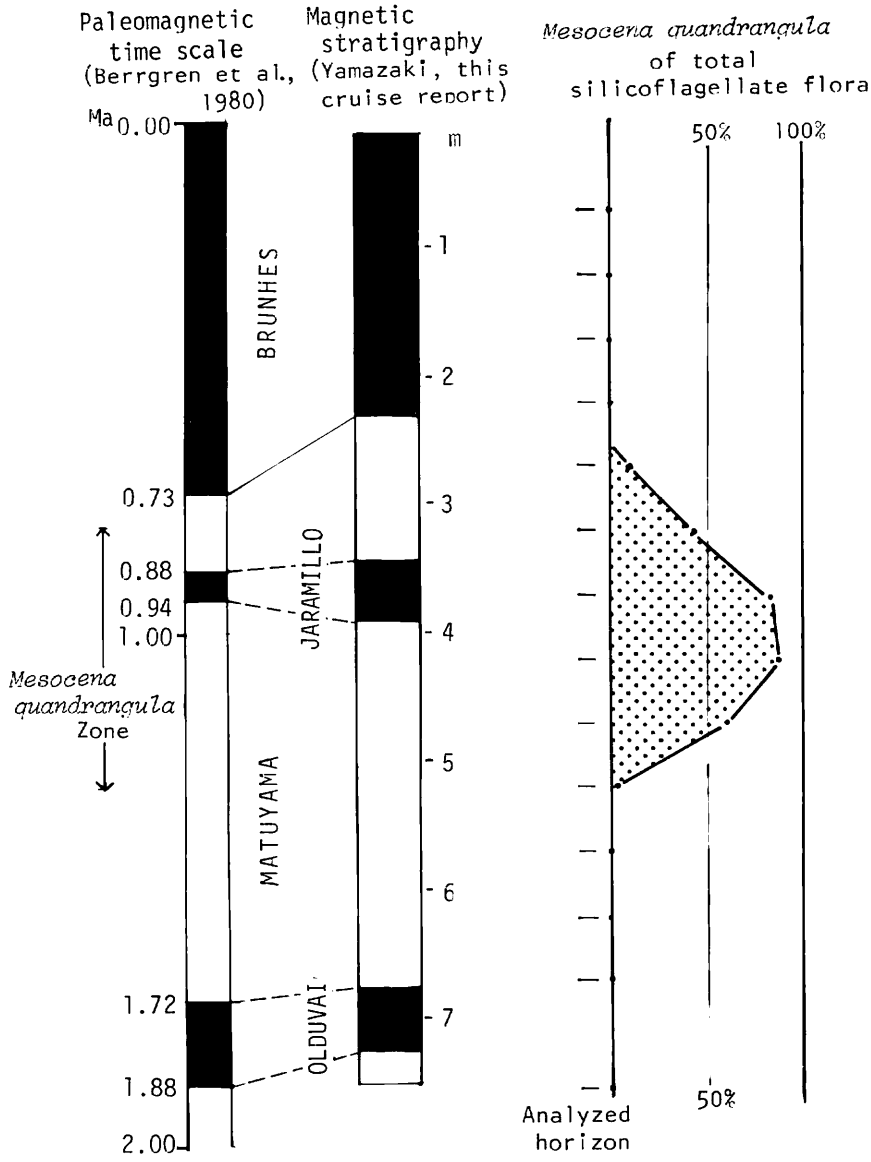


Fig. VI-8 Occurrence of *Mesocena quandrangula* EHRENBERG in Core P222.

geochronologic calibration of latest Oligocene to Pliocene radiolarian events, Equatorial Pacific. *Marine Micropaleontology*, 3, p. 377-395.

ZHUZE, A. P. and MUKHINA, V. V. (1973) The Mesocena elliptica EHR. zone in the Pleistocene sediments of the Pacific Ocean. *Okeanology*, 13(3), p. 386-394.

Table VI-3 Radiolarian occurrences and age assignments of some core and box core samples.

| Sample NO. & depth(cm) | Identified radiolarians | Age assignment ( Ma ) |
|---|---|---|
| P218 - 563 | *Pterocanium prismatium* Riedel<br>*Ommatartus penultimus* (Riedel) | 3.6 - 4.7 |
| P219 - 581 | *Pterocanium prismatium* Riedel<br>*Solenosphaera omnituba* Riedel and Sanfilippo<br>*Stichocorys peregrina* (Riedel) | 4.3 - 4.7 |
| P227 - 680 | *Ommatartus penultimus* (Riedel)<br>*Acrobotrys tritubus* Riedel<br>*Solenosphaera omnituba* Riedel and Sanfilippo | 4.9 - 6.4 |
| - 730 | *Ommatartus antepenultimus* Riedel and Sanfilippo<br>*Acrobotrys tritubus* Riedel | 5.5 -10.5 |
| - 766 | *Ommatartus antepenultimus* Riedel and Sanfilippo<br>*Cannartus laticonus* Riedel<br>*Ommatartus hughesi* (Cambell and Clark) | 8.0 -10.7 |
| P223 - 390 | *Solenosphaera omnituba* Riedel and Sanfilippo<br>*Ommatartus penultimus* (Riedel)<br>*Ommatartus antepenultimus* Riedel and Sanfilippo | 4.3 - 5.5 |
| - 440 | *Ommatartus hughesi* (Cambell and Clark)<br>*Cannartus laticonus* Riedel<br>*Dictyocoryne ontongensis* Riedel and Sanfilippo | 10.5 -11.2 |
| - 725 | *Cannartus laticonus* Riedel<br>*Dictyocoryne ontongensis* Riedel and Sanfilippo<br>*Lithopera thornburgi* Sanfilippo and Riedel | 10.5 -11.2 |
| P220 - 298 | *Dictyocoryne ontongensis* Riedel and Sanfilippo | 10.5 -11.2 |
| - 766 | *Dorcadospyris alata* (Riedel) | 11.1 -15.5 |
| P224 - 749 | *Cannartus tubarius* Haeckel<br>*Lychnocanoma elongata* (Vinassa) | 20.7 -23.2 |
| P225 - 720 | *Cannartus tubarius* Haeckel<br>*Lychnocanoma elongata* (Vinassa) | 20.7 -23.2 |
| B 60-bottom | *Lychnocanoma elongata* (Vinassa)<br>*Dorcadospyris forcipata* Haeckel<br>*Cannartus prismaticus* (Haeckel) | ca. 20 |
| B 64-bottom | *Spongaster pentas* Riedel and Sanfilippo<br>*Spongaster tetras* Ehrenberg | 3.4 - 3.6 |

## Supplement 2.
## SOME PECULIAR SEDIMENT COMPONENTS IN SEDIMENT SAMPLES OBTAINED DURING THE GH81-4 CRUISE, THE CENTRAL PACIFIC BASIN

### Manganese rich sediments

In uppermost part of Core P218, black micronodule concentrated layers with several centimeters thick are intercalated. The compositions of the sediments of black layers are mainly manganese micronodules and radiolarian tests. And these layers include some large manganese concretions with tube and irregular shapes (USUI, this cruise report). Most of radiolarian tests are attatched to small manganese oxide on their surfaces (Fig. VI-9). The shapes of manganese oxide are subspherical aggregation of fairly large individual crystals, compared with that of some other micronodules usually found in surface sediments which has origin of hydrogeneous and diagenous. The chemical composition of this layer is characterized by high content of manganese and nickel and low content of copper (MITA and NAKAO, this cruise report). Hydrother-

mal origin is suggested by its purity of manganese oxide and large crystals but further research is needed to explain formation mechanism of pure manganese oxide with high content of nickel and low content of cupper.

**Barite**

Euhedral crystals are abundantly occurred below the hiatus of Core P225 (Fig. VI-9). The crystals are identified to barite ($BaSO_4$) through the X-ray diffraction analysis by NAKAO who is the editor of this report. The occurrence of barite crystals is restricted within 30 centimeters below the hiatus and the dimension of barite crystals is $40 \times 20\ \mu m$ in mode and $90 \times 25\ \mu m$ in maximum. Barite in marine environments have been often reported related to hydrothermal mineralization. And microcrystals of barite are also suspended in water column and concentrated in sediments through organic activities. In equatorial eastern Pacific, sediments with high content of barite are widely distributed, and small crystals ($4 \times 2\ \mu m$) are common in these area (CHURCH, 1979). The barite crystals of Core P225 are peculiarly large and abundant. Restricted occurrence near the hiatus suggests the origin related to chemical environmental change caused by bottom water forming the hiatus.

## Reference

CHURCH, T. M. (1979) Marine barite.: BURNS, R. G. (ed.) Marine minerals. *Mineral. Soc., Amer., Short Course Notes*, 6, p. 175-209.

Fig. VI-9 Photographs of manganese oxides and barite crystals. 1, 2, and 7 are transmitted light micrographs and others are scanning electron micrographs.
single bar = 70 $\mu m$ double bar = 10 $\mu m$

1. Radiolarian species *Euchitonia furcata* EHRENBERG with some manganese oxide aggregations (Core P218, 40 cm).
2. Radiolarian species *Spongaster tetras* HAECKEL with some manganese oxide aggregations (Core P218, 40 cm).
3. Same as 2(Core P218, 40 cm).
4. Enlarged view of 3(Core P218, 40 cm). Manganese oxide aggregation on test.
5. Radiolarian species *Heliodiscus asteriscus* HAECKEL with some manganese oxide aggregations (Core P218, 40 cm).
6. Enlarged view of 5(Core P218, 40 cm). Manganese oxide aggregation around a broken spine.
7. Smear slide of barite crystal bearing siliceous ooze (Core P225, 280 cm).
8. Euhedral barite crystals (Core P225, 280 cm).
9. Enlarged view of single crystal (Core P225, 280 cm).

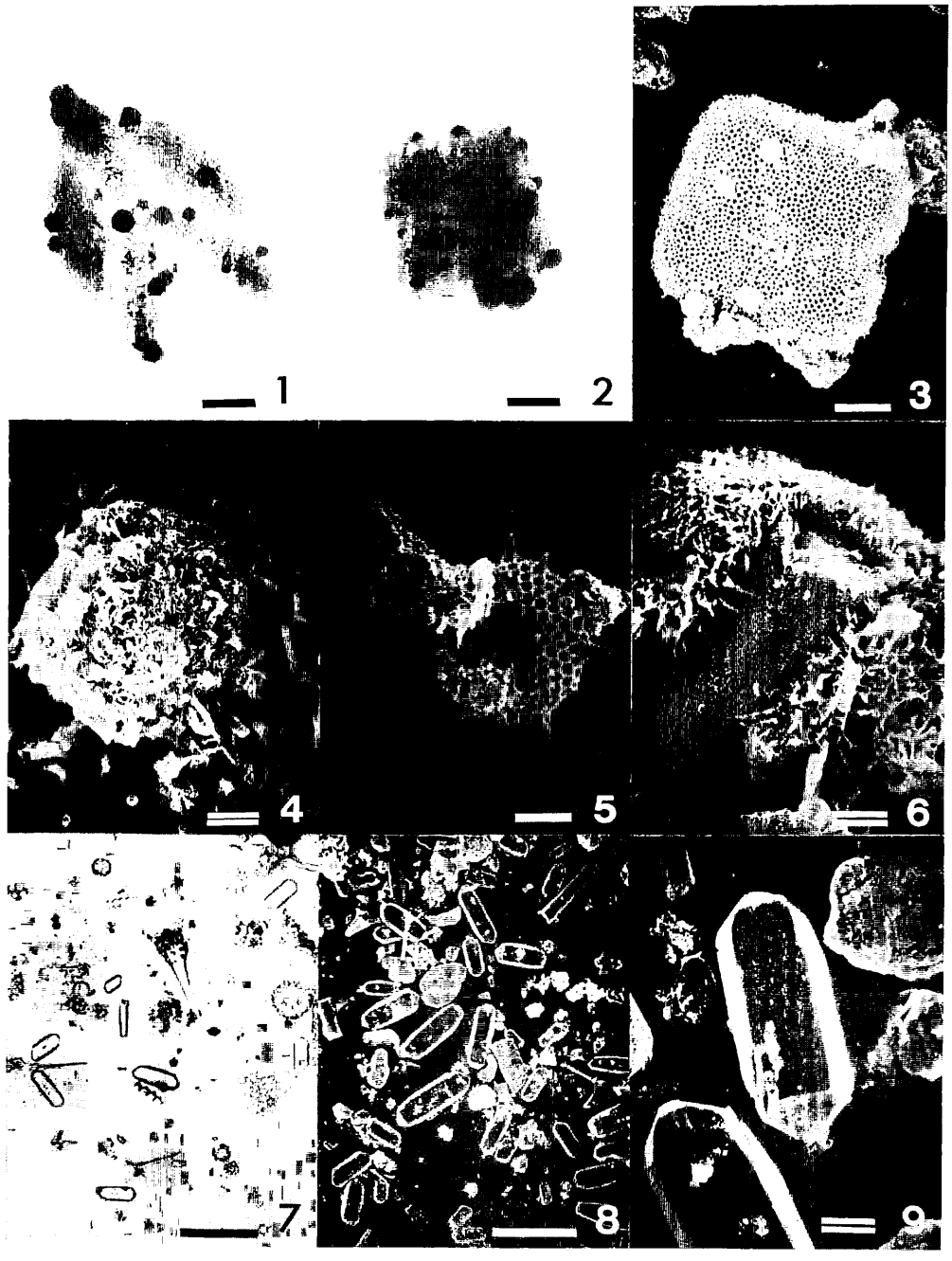
1
2
3
4
5
6
7
8
9